# Spin polarization and spin alignment in hypernuclei

H. Ejiri, T. Fukuda, and T. Shibata
*Department of Physics, Osaka University, Toyonaka, Osaka 560, Japan*

H. Bandō
*Division of Mathematical Physics, Fukui University, Fukui 910, Japan*

K.-I. Kubo
*Department of Physics, Tokyo Metropolitan University, Setagaya-ku, Tokyo 158, Japan*
(Received 15 December 1986)

Spin polarization and spin alignment of angular momenta in hypernuclei are discussed in terms of a distorted wave Born approximation. Hypernuclei produced by $(\pi^+,K^+)$ and $(K^-,\pi^-)$ reactions are shown to have sizable amounts of polarization and alignment. They are promising for use in spectroscopic studies of electromagnetic transitions, electromagnetic moments, and weak decays of hypernuclear states.

## I. INTRODUCTION

Strangeness exchange $(K^-,\pi^-)$ and $(\pi^+,K^+)$ reactions have been used to produce hypernuclear states.[1] Recently gamma decays and weak decays have been studied by measuring the decay particles from hypernuclear states produced by the $(K^-,\pi^-)$ reaction.[2–4] Spectroscopic studies of angular correlations are very important for further steps of the hypernuclear physics. Spin polarization and/or spin alignment are essential for such spectroscopic studies.[5,6] In particular, angular distributions of weak decay particles from polarized hypernuclei are used to study the weak decay mechanism and electromagnetic moments. The present work aims to report possible spin polarization and spin alignment in hypernuclear states produced by $(\pi^+,K^+)$ and $(K^-,\pi^-)$ reactions. A brief report on the polarization and the alignment in hypernuclei has been presented elsewhere.[7]

The angular momentum polarization of the hypernuclear state is produced in two ways. One is due to the distortions (absorptions) of the initial (projectile) wave and the final (ejectile) one, and the other is due to the spin dependent elementary process of the strangeness exchange reaction. The $K^-$, $\pi^-$, and $\pi^+$ involved in the $(K^-,\pi^-)$ and $(\pi^+,K^+)$ reactions are strongly absorbed in nuclei with mean free paths around $\lambda(\pi^\pm)\approx\lambda(K^-)\approx 2$ fm, while the $K^+$ is moderately absorbed with $\lambda(K^+)\approx 4$ fm.[8–12] Such absorptions give rise to the polarization of the orbital angular momenta introduced by the $(K^-,\pi^-)$ and $(\pi^+,K^+)$ reactions. The elementary process of the $(K^-,\pi^-)$ reaction at $P(K^-)=0.6$–$0.8$ GeV/$c$ produces little spin polarization of the hyperon.[13,14] while that of the $(\pi^+,K^+)$ one at $P(\pi^+)\approx 1$ GeV/$c$ produces a well-polarized hyperon.[15–19] Therefore, the polarization for hypernuclear states produced by the $(K^-,\pi^-)$ reaction is due to the polarization of the transferred orbital angular momentum, while that in the case of the $(\pi^+,K^+)$ reaction is composed of both the polarization of the orbital angular momentum and that of the intrinsic hyperon spin.

The angular momentum transferred to the hypernuclear state is aligned in a plane perpendicular to the recoil (transferred momentum) axis, preferentially along the axis normal to the reaction plane in the $(\pi^+,K^+)$ case.

General expressions for the transition amplitude of the reaction and for the orientation of the angular momentum are given in Sec. II. In Sec. III we describe polarization of the orbital angular momentum in hypernuclei in terms of a distorted wave Born approximation (DWBA). They are compared with evaluations based on a classical model and an eikonal approximation in Sec. IV. Overall polarizations and alignments, including the polarization of the intrinsic $\Lambda$ spin in the elementary process, are discussed in Sec. V, and concluding remarks are given in Sec. VI.

## II. PROBABILITY OF ORBITAL ANGULAR MOMENTUM ORIENTATION

The transition amplitude of the reaction $A(a,b)B$ is given by

$$\begin{aligned} T_{fi} &= \langle \mathbf{k}_b, J_B M_B, S_b m_b \mid V \mid \mathbf{k}_a, J_A M_A, S_a m_a \rangle \\ &= \Sigma_{lsj} (2j+1)^{1/2} A_{lsj} (J_A j M_A M_B - M_A \mid J_B M_B) \\ &\quad \times \beta_{sj}^{l m m_b m_a}(\mathbf{k}_b, \mathbf{k}_a) \, . \end{aligned} \tag{1}$$

Here we use the same notations for the spins and the reduced amplitude as used by Satchler.[20] For our $(\pi^+,K^+)$ and $(K^-,\pi^-)$ reactions on the zero-spin target nucleus, the above expression takes the following simple form,

$$T_{fi} = (2l+1)^{1/2} A_l \beta_{lm}(\mathbf{k}_b, \mathbf{k}_a) \, , \tag{2}$$

where $l$ and $m$ are the transferred orbital angular momentum and its projection to the $z$ axis, respectively.

 

In the conventional DWBA frame (0′ frame), the amplitude is described by taking the $z'$ axis along the incident momentum $\mathbf{k}_a$. The scattering plane is the $z'x'$ plane with the $y'$ axis parallel to $\mathbf{k}_a \times \mathbf{k}_b$. On the one hand, the polarization frame (0 frame) is defined as the $z$ axis parallel to $\mathbf{k}_a \times \mathbf{k}_b$ with the $x$ axis along $\mathbf{k}_a$. Hence, the two reduced amplitudes $\beta_{lm'}(\theta)$ of the 0′ frame and $\beta_{lm}(\theta)$ of the 0 frame are related through the rotation matrix[21]

$$\beta_{lm}(\theta)=\Sigma_{m'} D^{l}_{mm'}(\alpha,\beta,\gamma)\beta_{lm'}(\theta) , \tag{3}$$

with the Euler angles $\alpha=0$, $\beta=\pi/2$, and $\gamma=\pi/2$. In Eq. (3), $\theta$ is the scattering angle.

The vector polarization of the transferred orbital angular momentum is defined as

$$P_{y'}(\theta)=\frac{\mathrm{Tr}(l_{y'}T_{0'}T_{0'}^{+})}{l\,\mathrm{Tr}(T_{0'}T_{0'}^{+})} \tag{4}$$

in the DWBA (0′) frame, and

$$P_z(\theta)=\frac{\mathrm{Tr}(l_z T_0 T_0^{+})}{l\,\mathrm{Tr}(T_0 T_0^{+})} \tag{5}$$

in the polarization (0) frame. In the above expressions, $l_{y'}$ ($l_z$) is the orbital-angular-momentum operator along the $y'$ ($z$) axis in the 0′ (0) frame, which is perpendicular to the $z'x'$ ($xy$) scattering plane, and $T_{0'}$ ($T_0$) is the transition matrix in the 0′ (0) -frame representation. The former definition of polarization is the so-called Madison convention,[22] and the latter definition is useful to make an intuitive description of the angular-momentum-orientation phenomena, as will be frequently used in this article.

Using the reduced amplitudes, the polarization can be expressed as follows

$$P_{y'}(\theta)=\frac{\Sigma_{m'}[(l-m')(l+m'+1)]^{1/2}\mathrm{Im}[\beta_{lm'}(\theta)\beta^{*}_{lm'+1}(\theta)]}{l\Sigma_{m'}|\beta_{lm'}(\theta)|^{2}} \tag{6}$$

$$P_z(\theta)=\frac{\Sigma_m m\,|\beta_{lm}(\theta)|^{2}}{l\Sigma_m|\beta_{lm}(\theta)|^{2}}=\frac{\Sigma_m m P_m(\theta)}{l} , \tag{7}$$

where $P_m(\theta)$ is referred to the $m$-substate population probability in the 0 frame.

In case that $P_m(\theta)$ is constant with respect to $m$, the orbital angular momentum is distributed isotropically, and thus has no particular orientation (polarization). The finite polarization is realized if the substate distribution is asymmetric as $P_m(\theta)\neq P_{-m}(\theta)$. The case where $P_m(\theta)$ is not constant (not isotropic) but is symmetric as $P_m(\theta)=P_{-m}(\theta)$ is referred to as the alignment of the angular momentum. The case with $P_m(\theta)=P_{-m}(\theta)=\delta_{ml}\cdot\frac{1}{2}$ corresponds to the maximum positive alignment.

## III. DWBA CALCULATION

Polarization of orbital angular momenta in hypernuclei produced by $(\pi^+,\mathrm{K}^+)$ and $(\mathrm{K}^-,\pi^-)$ reactions are calculated by using the DWBA. Transition amplitudes are evaluated by using the following assumptions and parameters:

(i) A $\delta(r)$-type spin-independent interaction is used for the conversion interaction of neutron to $\Lambda$ particle.

(ii) Projectiles and ejectiles are described by the distorted waves with absorption. The absorption strengths for $\pi$ and K are determined from $\pi$N and KN total cross sections, respectively.[11]

(iii) The bound state wave functions of n and $\Lambda$ are obtained by using a Woods-Saxon potential.

(iv) The relativistic effect is taken into account for the distorted waves by using the energy dependent Schrödinger equation derived from the Klein-Gordon (KG) equation.[23]

Calculations were made for the following two typical cases:

(1) $[(1f_{\frac{7}{2}})_n^{-1}(1d_{\frac{5}{2}})_\Lambda]_{5^-}$ state in $^{56}_{\Lambda}$Fe populated by the $^{56}$Fe$(\pi^+,\mathrm{K}^+)$ reaction at $P(\pi^+)=1.05$ GeV/$c$.

(2) $[(1f_{\frac{7}{2}})_n^{-1}(1d_{\frac{5}{2}})_\Lambda]_{1^-}$ state in $^{56}_{\Lambda}$Fe populated by the $^{56}$Fe$(\mathrm{K}^-,\pi^-)$ reaction at $P(\mathrm{K}^-)=0.72$ GeV/$c$. These momenta are often used to excite $\Lambda$ hypernuclei because of large cross sections for the n$\rightarrow\Lambda$ conversion. Then the $(\pi^+,\mathrm{K}^+)$ reaction is characterized by the large momentum transfer of $q\approx 0.35$ GeV/$c$ and thus the large angular momentum transfer of around $l\hbar\sim 3-10\hbar$, while the $(\mathrm{K}^-,\pi^-)$ by the small one of $q\lesssim 0.05$ GeV/$c$ and $l\hbar\lesssim 1\hbar$.

The assumption of the spin-independent interaction is approximately valid for the $(\mathrm{K}^-,\pi^-)$ reaction with almost no spin-flip process.[13,14] In the $(\pi^+,\mathrm{K}^+)$ reaction with a large $\Lambda$-spin polarization the spin-flip process[15–19] has to be added to the calculated orientation of the orbital angular momentum (see Sec. V), but may not be important for the present calculation of the polarization of the orbital angular momentum.

The $[(1f_{\frac{7}{2}})_n^{-1}(1d_{\frac{5}{2}})_\Lambda]_{5^-}$ state is expected to be strongly populated by the $^{56}$Fe$(\pi^+,\mathrm{K}^+)^{56}_{\Lambda}$Fe reaction at $P(\pi^+)=1.05$ GeV/$c$ because of the best matching transferred $l=5$ and of the large radial-overlap integral.[24] Imaginary potential strengths are obtained from the total cross sections of $\langle\sigma_t\rangle_\pi=41$ mb and $\langle\sigma_t\rangle_{\mathrm{K}}=14$ mb for the $\pi^+$ and $\mathrm{K}^+$ mesons, respectively. Calculated angular distributions for the differential cross section $d\sigma/d\Omega$ and the polarization $P(\theta)$ are shown in Fig. 1(a). In order to see the polarization mechanism the calculated distributions are decomposed into the near-side ($N$) and far-side ($F$) reaction processes,[25] as shown in Fig. 2. Calculations show clearly the large positive $P(\theta)$ for the far-side process, the large negative $P(\theta)$ for the near-side process, the large excess of $d\sigma^N(\theta)/d\Omega$ for the near-side process over $d\sigma^F(\theta)/d\Omega$ for the far-side one, and finally the moderate amount of the overall $P(\theta)$. The large polarization of around $P(\theta)=-0.3$ to $-0.4$ are obtained at $\theta=20°-30°$.

The $(\mathrm{K}^-,\pi^-)$ reaction at $P(\mathrm{K}^-)=0.72$ GeV/$c$ favors low angular momentum transfer. The total cross sections used to extract the imaginary potential strengths are $\langle\sigma_t\rangle_\pi=\langle\sigma_t\rangle_{\mathrm{K}}=30$ mb. Calculated $d\sigma(\theta)/d\Omega$ and $P(\theta)$ for the $[(1f_{\frac{7}{2}})_n^{-1}(1d_{\frac{5}{2}})_\Lambda]_{1^-}$ state populated by the

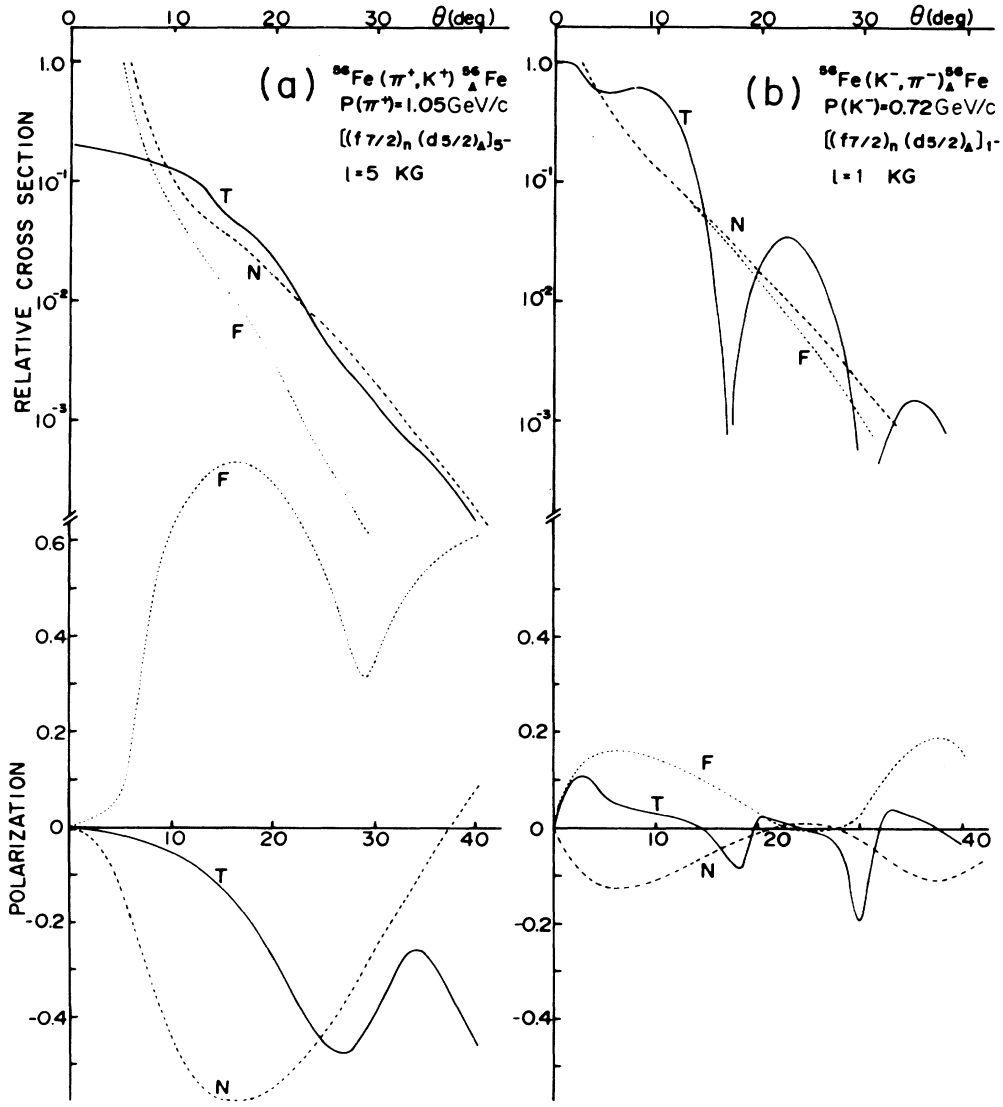


FIG. 1. (a) DWBA calculation for the $^{56}$Fe$(\pi^+,K^+)^{56}_{\Lambda}$Fe reaction at $P(\pi^+)=1.05$ GeV/$c$, leading to the $[(1f\frac{7}{2})_n^{-1}(1d\frac{5}{2})_\Lambda]_{5^-}$ state. Top: Differential cross-sections. Bottom: Polarization of the orbital angular momentum. Dashed lines with $N$ and dotted lines with $F$ are the near-side and far-side contributions, respectively, and solid lines with $T$ are for the coherent sum of these contributions. (b) DWBA calculation for the $^{56}$Fe$(K^-,\pi^-)$ reaction leading to the $[(1f\frac{7}{2})_n^{-1}(1d\frac{5}{2})_\Lambda]_{1^-}$ state at $P(K^-)=0.72$ GeV/$c$. See caption for (a). The scattering angles $\theta$ (in deg) are given on the horizontal axis.

$^{56}$Fe$(K^-,\pi^-)^{56}_{\Lambda}$Fe reaction are shown in Fig. 1(b). They are quite different from those for the $(\pi^+,K^+)$ reaction. The far-side and near-side processes have positive and negative polarizations, respectively, but their absolute values are small. The cross sections for the near-side and the far-side processes, however, are nearly the same. Therefore the overall polarization must be influenced by the interference between the near-side and far-side amplitudes. The overall polarization is positive, and is rather small, 10% at forward angles.

## IV. CLASSICAL MODEL AND EIKONAL APPROXIMATION

It is interesting to evaluate the polarization in terms of a schematic classical model in order to get an intuitive view. In the classical model the interaction region contributing to the positive polarization and that to the negative one are divided by a line along the transferred momentum q, as shown in Fig. 2. Then the polarization depends on which contribution is larger than the other.

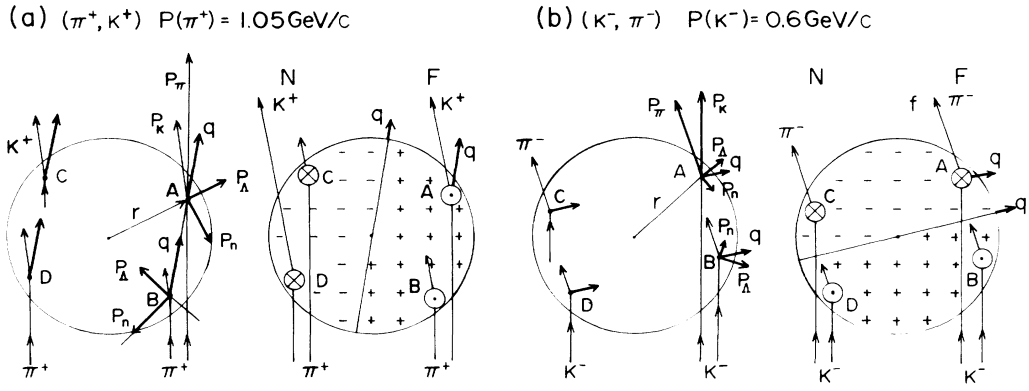


FIG. 2. Schematic reaction diagrams for the polarization mechanism of Λ hypernuclear production. ⊙ and ⊗ indicate the upward and downward polarizations, respectively. $N$ and $F$ denote the near-side and the far-side reactions, respectively. $A$, $B$, $C$, and $D$ stand for the effective interaction points. $q$ is the transferred momentum. + and − stand for the interaction regions contributing to the positive and negative polarizations, respectively. (a) $(\pi^+,\mathrm{K}^+)$ reaction with a large momentum transfer $q$. $P_n$ and $P_\Lambda$ are momenta of the neutron and the Λ hyperon in the $n\rightarrow\Lambda$ process, respectively, and $r$ is the effective interaction radius. (b) $(\mathrm{K}^-,\pi^-)$ reaction with a small momentum transfer. For both (a) and (b), $\mathbf{P}_\Lambda$ for Λ in $s$ state with $\boldsymbol{l}_\Lambda=\mathbf{r}\times\mathbf{P}_\Lambda=0$ are drawn.

In the case of the $(\pi^+,\mathrm{K}^+)$ reaction with the large longitudinal **q**, the division coincides nearly with the division of the near-side and far-side reactions. Since the near-side contribution is less attenuated than the far-side one because of the shorter path length, the near-side contribution and, accordingly, the negative polarization become larger than the other. The polarization of the orbital angular momentum is evaluated in terms of the schematic classical model as described in detail in the Appendix. The classical model calculation agrees well with the DWBA calculation as shown in Fig. 3.

In the case of the $(\mathrm{K}^-,\pi^-)$ reaction with the small transversal **q**, the positive polarization region is the upstream (projectile-side) region rather than the far-side region, and similarly the negative polarization region is the downstream (ejectile-side) region. Consequently the polarization depends on the attenuation (absorption) of the projectile relative to that of the ejectile. Actually the polarization is shifted towards negative by setting the mean free path $\lambda_K=\infty$ (no projectile attenuation) and towards positive by setting $\lambda_\pi=\infty$ (no ejectile attenuation).

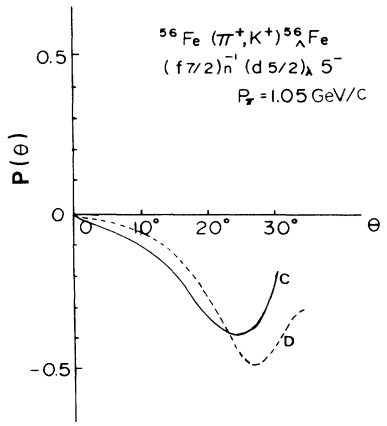


FIG. 3. Polarization of the orbital angular momentum for the $[(1f_{\frac{7}{2}})_n^{-1}(1d_{\frac{5}{2}})_\Lambda]_{5^-}$ state produced by the $^{56}\mathrm{Fe}(\pi^+,\mathrm{K}^+)^{56}_\Lambda\mathrm{Fe}$ reaction at $P(\pi^+)=1.05$ GeV/$c$. The solid line $C$ and dashed line $D$ are the classical model and DWBA calculations, respectively.

Since major distortion potentials for π and K mesons are the imaginary (absorption) potentials $W(\pi)$ and $W(\mathrm{K})$, the polarization can be evaluated by employing the distorted-wave impulse approximation (DWIA) together with the eikonal approximation for the meson distorted waves. The calculation for the $(\pi^+,\mathrm{K}^+)$ reaction at $P(\pi^+)=1.05$ GeV/$c$ gives negative polarization, consistent with the DWBA calculations and the classical model. The case of the $(\mathrm{K}^-,\pi^-)$ reaction, however, is quite delicate, being sensitive to the relative absorption strength of the projectile and ejectile. Polarizations of the $[(1p_{\frac{3}{2}})_n^{-1}(1s_{\frac{1}{2}})_\Lambda]_{1^-}$ state produced by the $^{12}\mathrm{C}(\mathrm{K}^-,\pi^-)$ reaction at $P(\mathrm{K}^-)=0.72$ GeV/$c$ are calculated by the DWIA with the eikonal approximation for various imaginary (absorption) potential parameters $W$. The polarization is found to depend strongly on the relative strengths of the $W(\mathrm{K}^-)$ and $W(\pi^-)$. The polarization is negative for $W(\mathrm{K}^-)<W(\pi^-)$ and increases as the ratio $W(\mathrm{K}^-)/W(\pi^-)$ increases. These features are just in accord with the classical model as discussed above.

## V. DISCUSSION

So far, orientation of the transferred orbital angular momenta $l$ introduced by momentum transfers in $(\pi^+,\mathrm{K}^+)$ and $(\mathrm{K}^-,\pi^-)$ reactions have been discussed. In order to evaluate orientation of total angular momenta, one has to take into account polarization of the intrinsic Λ spin $\mathbf{s}_\Lambda$ and coupling of $\mathbf{s}_\Lambda$ to $\boldsymbol{l}_\Lambda$.

The elementary (nucleon) process of $\pi^- + p \rightarrow K^0 + \Lambda$ is experimentally known to give a large positive polarization of the $\Lambda$ spin at $P_\pi \approx 1$ GeV/$c$.[15-19] Thus the conjugate process of $n(\pi^+, K^+)\Lambda$ must give also large polarization of $\Lambda$ with positive sign at that incident momentum, where the $(\pi^+, K^+)$ reaction is used for producing $\Lambda$ hypernuclei. The $\Sigma$ hyperon is also polarized at that incident momentum.[15-19] As shown in Fig. 4, the $\Lambda$ spin is polarized along the direction of $\mathbf{P}_\pi \times \mathbf{P}_K$ (quantization axis $z$) with the polarization $P_\Lambda = 0.5$–$0.8$. We discuss first a simple case of the odd $A$ target nucleus with an odd neutron in the $j_n = l_n \pm \frac{1}{2}$ orbit. Since the $(\pi^+, K^+)$ reaction gives a large angular momentum transfer $l$ with $m \approx \pm l$, the neutron with $l_n$ and its $z$ component of $m_n = \pm l_n$ is likely to be converted to the $\Lambda$ with $l_\Lambda = l - l_n$ and $m_\Lambda = \mp l_\Lambda$, where the upper and lower signs of $m_\Lambda$ correspond to the transferred component of $m = -l$ (near side) and $m = +l$ (far side), respectively. Consequently the $(\pi^+, K^+)$ reaction gives $j_\Lambda = l_\Lambda - \frac{1}{2}$ in the case of the near-side process, and $j_\Lambda = l_\Lambda + \frac{1}{2}$ in the case of the far-side process, both with the intrinsic $\Lambda$ spin upward. If they are particle-bound excited states, electric $\gamma$ transitions finally feed the ground state with the $\Lambda$ in the $s$ orbit. Then the intrinsic $\Lambda$ spin remains upward. In case of the $(p\frac{3}{2})_n \rightarrow (s\frac{1}{2})_\Lambda$ in the $^9$Be$(\pi^+, K^+)$ reaction, as shown in Fig. 4(a), both the near-side and far-side processes lead to the ground state with the intrinsic $\Lambda$ spin upward.

The polarization of the $[(1f\frac{7}{2})_n^{-1}(1s\frac{1}{2})_\Lambda]_{J^-}$ state produced by the $^{56}$Fe$(\pi^+, K^+)$ reaction is shown in Fig. 4(b). The near-side reaction leads to the downward spin $3^-$ state with $[j_n', j_\Lambda]_{3^-}$, while the far-side one leads to the upward spin $4^-$ state with $[j_n', j_\Lambda]_{4^-}$, where $j_n'$ is the total spin of the last uncoupled neutron in the hypernucleus. Both leave the $\Lambda$ with the upward intrinsic spin. The negative polarization due to the favorable (less-absorptive) near-side reaction means that the population of $3^-$ is larger than that of $4^-$. In the lower excitation region of $^{56}_{\Lambda}$Fe there are states $[j_n'(2p\frac{3}{2})j_\Lambda(1s\frac{1}{2})]_J$ with $J^\pi = 2^-$ and $1^-$. Thus the $4^-$ and $3^-$ states decay by $E2$ $\gamma$ transitions to the $2^-$ and $1^-$ states, respectively. Thereby the $\Lambda$ spin is not affected much. One of the $2^-$ and $1^-$ states lies higher than the other. Thus, it decays by $M1$ transition, which induces some depolarization. Thus the polarization of the intrinsic $\Lambda$ spin in the ground state may be reduced by a factor of about $\frac{1}{2}$ from that in the $3^-$ or $4^-$ state.

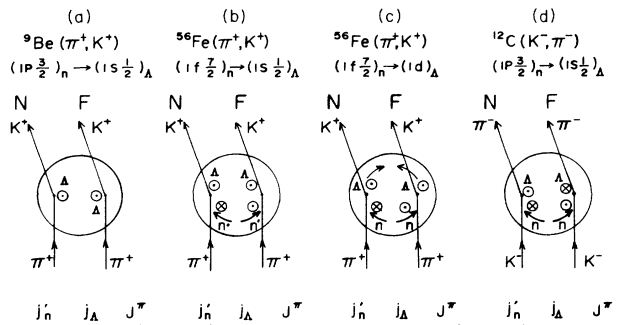


FIG. 4. Schematic diagram of polarization of hypernuclei produced by $(\pi^+, K^+)$ and $(K^-, \pi^-)$ reactions, in which a neutron with $j_n$ is converted to a $\Lambda$ hyperon with $j_\Lambda$. Configuration of the orbital angular momentum and the intrinsic nucleon ($\Lambda$) spin in the hypernucleus is given at the bottom, in which $j_n'$ and $j_\Lambda$ stand for angular momenta of the neutron and the $\Lambda$ in the hypernuclear state, respectively, and $J^\pi$ stands for the total angular momentum and the parity. See also captions in Fig. 2.

Polarizations of high spin states with the $[(1f\frac{7}{2})_n^{-1}(1d\frac{5}{2})_\Lambda]_{6^-}$ and the $[(1f\frac{7}{2})_n^{-1}(1d\frac{3}{2})_\Lambda]_{5^-}$ configurations in $^{56}_{\Lambda}$Fe populated by the $(\pi^+, K^+)$ reaction are shown in Fig. 4(c). The near-side and the far-side reactions feed $5^-$ and $6^-$ states, respectively. Here the $5^-$ state with the negative polarization is favored. These $5^-$ and $6^-$ states are below the threshold energy of the $\Lambda$ emission, but well above the threshold energy of the neutron emission. Then the $\Lambda$ deexcites to lower $\Lambda$ orbits while neutrons are excited to higher levels through $\Lambda$-n interactions (collisions) in $^{56}_{\Lambda}$Fe, and the hypernucleus decays by emitting one neutron to $^{55}_{\Lambda}$Fe. If the nucleon-spin $\Lambda$-spin interaction is small, the $\Lambda$-spin polarization is still maintained after the nucleon emission, and one gets the ground state in $^{55}_{\Lambda}$Fe with the intrinsic $\Lambda$ spin polarized upward, provided that electric $\gamma$ transitions in $^{55}_{\Lambda}$Fe are dominant.

The elementary process of the $(K^-, \pi^-)$ reaction at around $P_K = 0.7$ GeV/$c$ is found to give little spin polarization.[13,14] We consider the $[(1p\frac{3}{2})_n^{-1}(1s\frac{1}{2})_\Lambda]_{1^-}$ state populated by the $^{12}$C$(K^-, \pi^-)$ reaction [Fig. 4(d)]. Since the $(K^-, \pi^-)$ elementary process is mainly of non-spin-flip, the natural parity state of $J^\pi = 1^-$ is preferentially excited in both the near-side and far-side reactions. Then the positive polarization of the orbital angular momentum indicates the positive polarization of the neutron spin and the negative one of the $\Lambda$ spin.

Angular momentum in hypernuclei introduced by momentum transfer of the $(\pi^+, K^+)$ or $(K^-, \pi^-)$ reaction is aligned in a plane perpendicular to the transferred momentum, preferentially along the axis normal to the reaction plane. In fact, the DWBA calculation for the $^{56}$Fe$(\pi^+, K^+)$ reaction indicates the large polarization for both the near-side and far-side reactions (see Fig. 1). The alignment may be disturbed in principle by particle or $\gamma$ deexcitation if the hypernuclear state is an unbound or excited state. The alignment, however, is fairly well preserved even after such deexcitation, particularly in case of the $(\pi^+, K^+)$ reaction with large $l$. This is because the angular momentum removed by each particle or $\gamma$ ray is much smaller than $l$, as the alignment of compound nuclei is well preserved even after evaporation of particles and emission of $\gamma$ rays.[26]

## VI. CONCLUDING REMARKS

This paper reports possible polarization and alignment of orbital angular momenta in hypernuclei. The DWBA

calculation predicts a large negative polarization of $P(\theta)=-0.2$ to $-0.4$ for orbital angular momenta of hypernuclear states produced by the $(\pi^+,K^+)$ reaction at $P(\pi^+)=1.05$ GeV/$c$. The polarization is semiquantitatively reproduced by the classical model calculation, in which absorption of both the projectile and the ejectile along their trajectories is taken into account. This is due to facts that the imaginary part dominates distorting potentials for both the projectile and the ejectile and that the linear and angular-momentum transfers are quite large. Similar arguments have been applied for evaluating analyzing powers of (p,$\pi$) reactions.[27]

The DWBA calculation for hypernuclear states produced by the $(K^-,\pi^-)$ reaction at $P_K=0.72$ GeV/$c$ predicts small positive polarization of $P(\theta)\approx 0.1$. Here the linear- and angular-momentum transfers are quite small and contributions from various geometrical reaction points (see Fig. 2) cancel out with each other, resulting in rather small polarization. Then the polarization is influenced by the interference between the amplitudes of the near-side and far-side reactions. In the $(K^-,\pi^-)$ reaction with the transverse momentum transfer, relative contributions of the upstream and downstream reactions are important. Thus, the sign of the overall polarization may depend also on the relative absorption strength of the projectile and the ejectile.

Since the elementary process of $\pi^+ + n \rightarrow K^+ + \Lambda$ gives a large polarization of the intrinsic $\Lambda$ spin, the polarization of the orbital angular momentum in the $(\pi^+,K^+)$ reaction is coupled with the polarization of the intrinsic $\Lambda$ spin. Proper choice of the $j_\Lambda = l_\Lambda \pm \frac{1}{2}$ and/or total $J$ leads to well-polarized $j_\Lambda$, $J$, and $s_\Lambda$.

Angular momenta of hypernuclei are aligned in a plane perpendicular to the transferred momentum. The large positive and negative polarizations for the far-side and near-side reactions, respectively, indicate the large alignment along the direction normal to the reaction plane.

Polarization and alignment of excited (unbound) hypernuclear states may be preserved to some extent even through $\gamma$ (or particle) deexcitation process.

Polarization and alignment of hypernuclear states, which are crucial for angular distribution studies of $\gamma$ rays and weak decay particles, are used for investigating electromagnetic transitions, the electromagnetic moment[28] and weak decay mechanisms.[6]

The authors thank Prof. H. Toki, Prof. T. Motoba, and Dr. H. Ohsumi for valuable discussions.

## APPENDIX: A CLASSICAL MODEL

It is interesting to evaluate the polarization of orbital angular momenta in hypernuclei produced by $(\pi^+,K^+)$ and $(K^-,\pi^-)$ reaction in a classical model. Let us first discuss the $(\pi^+,K^+)$ reaction [Fig. 2(a)].

The $K^+$ momentum $\mathbf{p}_K$ and the momentum transfer $\mathbf{q}$ are given as $\mathbf{q}=\mathbf{p}_\pi-\mathbf{p}_K=\mathbf{p}_\Lambda-\mathbf{p}_n$, where $\mathbf{p}_n$ and $\mathbf{p}_\Lambda$ are the momentum of the neutron and that of the $\Lambda$, respectively. The angular momentum transfer is written as $\boldsymbol{l}\hbar=\boldsymbol{l}_\Lambda\hbar-\boldsymbol{l}_n\hbar=\mathbf{r}\times\mathbf{q}$, where $\mathbf{r}$ is the effective interaction point from the center of the nucleus. The effective radius is evaluated as the radius where the initial state $\psi_n$ and the final one $\psi_\Lambda$ overlap well. There are four effective interaction points $A$, $B$, $C$, and $D$, as shown in Fig. 2(a), which satisfy matching conditions of both the momentum and the angular momentum for the given transition of $l_n \rightarrow l_\Lambda$ and the given scattering angle $\theta$. Here reactions are assumed to take place in the equatorial plane (see Fig. 2), where angular momenta involved are simply $m_\pi=\pm l_\pi$, $m_K=\pm l_K$, and $m=\pm l$ by taking the quantization axis ($z$ axis) normal to the reaction plane. These angular momenta compose a stretched configuration of $l_\pi=l_K+l$, leading to the best $l$-matched reaction. Reactions at the nonequatorial plane introduce nonstretched coupling of $\boldsymbol{l}_\pi$, $\boldsymbol{l}_K$, and $\boldsymbol{l}$, resulting necessarily in decrease of the reaction amplitude by the coupling coefficient. Furthermore, $l_\pi$ and $l_K$ in the nonstretched coupling for given $l$ deviate from the optimum values. The transition amplitudes are decomposed into near-side ($N$) and far-side ($F$) contributions.[25] Then $A$ and $B$ belong to the far-side scattering, and $C$ and $D$ to the near-side scattering. Defining the direction of the polarization vector as in Sec. II, $A$ and $B$ give positive polarization of $l$ and $C$ and $D$ negative polarization.

The polarization is expressed as

$$P(\theta)=\frac{\sigma^N(\theta)P^N(\theta)+\sigma^F(\theta)P^F(\theta)}{\sigma^N(\theta)+\sigma^F(\theta)}\ , \tag{A1}$$

where $\sigma^N(\theta)$ and $\sigma^F(\theta)$ are cross sections for the near-side and far-side reactions, respectively, and $P^N(\theta)$ and $P^F(\theta)$ are the corresponding polarizations. The interference arising from the quantum effect is not taken into account in Eq. (A1). By using $\sigma^i(\theta)$ for the contribution from the point $i=A$, $B$, $C$, and $D$, one can write $\sigma^N(\theta)=\sigma^C(\theta)+\sigma^D(\theta)$ and $\sigma^F(\theta)=\sigma^A(\theta)+\sigma^B(\theta)$. As shown in Fig. 2(a), one may set $P^F(\theta)\approx -P^N(\theta)\approx 1$ in the equatorial plane. Actually the contribution from the nonequatorial plane decreases much as discussed above. Thus, $P^F(\theta)$ and $-P^N(\theta)$ may not deviate much from 1. The cross section is assumed to be proportional to the attenuation factor $\exp(-t_K^i/\lambda_K - t_\pi^i/\lambda_\pi)$, where $t_K^i$ and $t_\pi^i$ are the path lengths of K and $\pi$ in the nuclear matter for the point $i$, respectively. Thus, the polarization is rewritten as

$$P(\theta)=\frac{R_{FN}(\theta)-1}{R_{FN}(\theta)+1}\ , \tag{A2}$$

$$R_{FN}(\theta)=\frac{\sigma^F(\theta)}{\sigma^N(\theta)}=\frac{\exp(-t_\pi^A/\lambda_\pi - t_K^A/\lambda_K)+\exp(-t_\pi^B/\lambda_\pi - t_K^B/\lambda_K)}{\exp(-t_\pi^D/\lambda_\pi - t_K^D/\lambda_K)+\exp(-t_\pi^C/\lambda_\pi - t_K^C/\lambda_K)}\ . \tag{A3}$$

The path lengths for the near-side reaction ($C$ and $D$ in Fig. 2) become shorter than the corresponding ones for the far-side reactions ($A$ and $B$), i.e., $t_K^D < t_\pi^A$, $t_\pi^D < t_K^A$, $t_\pi^C < t_K^B$, and $t_K^C < t_\pi^B$, as the outgoing particle bends more towards the near side. Thus, the near-side reaction is less attenuated by the absorption than the far-side one. Consequently, one gets $R_{FN}(\theta) < 1$ and the negative polarization $P(\theta) < 0$. Since $\lambda_K$ for $K^+$ is almost twice $\lambda_\pi$ for $\pi^+$, the polarization is somewhat weakened.

The polarization for the $^{56}$Fe$(\pi^+,K^+)^{56}_{\Lambda}$Fe reaction is evaluated by using the Eq. (A2). The transition considered is $(1f)_n \rightarrow (1d)_\Lambda$. It has a large overlap between $\psi_n$ and $\psi_\Lambda$. The effective interaction radius is evaluated as $r \approx 4$ fm from the overlap of $\psi_n$ and $\psi_\Lambda$. The meson momenta are $P_\pi = 1.05$ GeV/$c$ and $P_K = 0.72$ GeV/$c$, with $\lambda_\pi = 2$ fm and $\lambda_K = 4.7$ fm, respectively.[8–12] The momentum transfer is $q = 0.35$–$0.5$ GeV/$c$ at $\theta = 0°$–$30°$, and corresponding $l = 4$–$10$. Thus, we take the maximum value of $l = 5$ for the $(1f)_n \rightarrow (1d)_\Lambda$, which gives the largest cross section.[24] Then the neutron in the $f$ orbit with the substate $m_n = \pm 3$ is kicked into the $d$ orbit of $\Lambda$ with the reversed direction of $m_\Lambda = \mp 2$. The evaluated result gives negative polarization as shown by the solid line in Fig. 3. The negative sign reflects indeed the smaller absorption (shorter path) for the near-side process than for the far-side one.

The $(K^-,\pi^-)$ reaction at $P(K^-) = 0.5$–$0.8$ GeV/$c$ has been extensively used for exciting low-spin $\Lambda$ hypernuclei because of the large cross section of the elementary process and of the small momentum transfer.[1] Here $\mathbf{q}$ is mostly transversal as shown in Fig. 2(b). In contrast to the $(\pi^+,K^+)$ reaction, the far-side reactions at $A$ and $B$ give negative and positive $l$ polarizations, respectively. Thus they cancel with each other, resulting in the small $P^F(\theta)$, and similarly cancellation of the polarizations at $C$ and $D$ results in the small $P^N(\theta)$ [see Fig. 2(b)]. Moreover, $P^F(\theta)$ and $P^N(\theta)$ may tend to cancel with each other. Therefore the overall polarization becomes quite small. In such case of cancellation the polarization may hardly be evaluated by a classical treatment since the interference term plays an important role for the polarization.


[1] Proceedings of the BNL International Symposium on Hypernuclear and Kaon Physics, 1985 [Nucl. Phys. **A450** (1986), and references therein].

[2] M. May *et al.*, Phys. Rev. Lett. **51**, 2085 (1983).

[3] P. D. Barnes *et al.*, Nucl. Phys. **A450**, 430c (1986).

[4] R. Grace *et al.*, Phys. Rev. Lett. **55**, 1055 (1985).

[5] A. Masaike and H. Ejiri, in Proceedings of the Third LAMPF II Workshop, 1983, Los Alamos National Laboratory Report LA 9933-CII, 1983, p. 823.

[6] T. Motoba, H. Bandō, K. Ikeda, and T. Yamada, Prog. Theor. Phys. Suppl. No. 81, 42 (1985); H. Bandō, Genshikaku-Kenkyu **31**, 99 (1986).

[7] H. Ejiri, T. Fukuda, T. Shibata, H. Bandō and K.-I. Kubo, in *Proceedings of the INS International Symposium on Hypernuclear Physics,* Tokyo, 1986, edited by H. Bandō, O. Hashimoto, and K. Ogawa (University of Tokyo, Tokyo, 1986).

[8] B. R. Martin, Nucl. Phys. **B94**, 413 (1975).

[9] M. Alston-Garnjost *et al.*, Phys. Rev. D **18**, 182 (1978).

[10] G. P. Gopal *et al.*, Nucl. Phys. **B119**, 362 (1977).

[11] C. B. Dover and G. E. Walker, Phys. Rev. C **19**, 1393 (1979); C. B. Dover, L. Ludeking, and G. E. Walker, *ibid.* **22**, 2073 (1980).

[12] D. Marlow *et al.*, Phys. Rev. C **25**, 2619 (1982).

[13] R. Armenteros *et al.*, Nucl. Phys. **B21**, 15 (1970).

[14] R. Armenteros *et al.*, Nucl. Phys. **B8**, 233 (1968).

[15] R. D. Baker *et al.*, Nucl. Phys. **B126**, 365 (1977).

[16] J. E. Rush, Jr., Phys. Rev. **173**, 1776 (1968).

[17] Y. S. Kim *et al.*, Phys. Rev. **151**, 1090 (1966).

[18] R. D. Baker *et al.*, Nucl. Phys. **B141**, 29 (1978).

[19] O. I. Dahl *et al.*, Phys. Rev. **163**, 1430 (1967).

[20] G. R. Satchler, Nucl. Phys. **55**, 1 (1964).

[21] D. M. Brink and G. R. Satchler, *Angular Momentum* (Oxford University Press, New York, 1962).

[22] H. H. Barshall and W. Haeberli, *Polarization Phenomena in Nuclear Reactions* (University of Wisconsin Press, Madison, 1971) p. xxv.

[23] E. H. Auerbach *et al.*, Ann. Phys. (N.Y.) **148**, 381 (1983).

[24] H. Bandō and T. Motoba, Prog. Theor. Phys. **76**, 1321 (1986).

[25] R. C. Fuller, Phys. Rev. C **12**, 1561 (1975).

[26] H. Ejiri, *et al.*, Phys. Lett. **18**, 314 (1965); Nucl. Phys. **89**, 641 (1966).

[27] H. Toki and K.-I. Kubo, Phys. Rev. Lett. **54**, 1203 (1985).

[28] T. Fukuda, H. Ejiri, T. Shibata, H. Bandō, and T. Motoba, in *Proceedings of the INS International Symposium on Hypernuclear Physics,* Tokyo, 1986, edited by H. Bandō, O. Hashimoto, and K. Ogawa, (University of Tokyo, Tokyo, 1986).